ENHANCED HUMAN KNEE CARTILAGE EVALUATION USING REDUCED INTERACTIVE SEGMENTATION MODEL

JOYCE SIA SIN YIN

A thesis submitted in fulfilment of the
requirements for the award of the degree of
Doctor of Philosophy

School of Biomedical Engineering and Health Sciences
Faculty of Engineering
Universiti Teknologi Malaysia

OCTOBER 2021

DEDICATION

Dear dad and mom, this is for you.

ACKNOWLEDGEMENT

I would like to express my heartiest appreciation to my supervisor, Assoc. Prof. Ir. Dr. Tan Tian Swee, who has been guiding me throughout the ups and downs during my study. He showed great passion for contributing ideas and motivation, pushing me to work harder by following my timeline strictly.

Besides, I would like to credit the completion of this thesis to my co-supervisors, who are Assoc. Prof. Ir. Dr. Azli Bin Yahya, Ir. Dr. Hum Yan Chai, Dr. Khairil Amir Bin Sayuti, and Dr. Ahmad Tarmizi Musa for assisting me at the results validation stages and also offering advices and guidance in publications.

I am also indebted to Universiti Teknologi Malaysia (UTM) for offering the Zamalah scholarship to support my living expenses during my study.

My fellow lab colleagues should also be recognised for their contributions and motivation. My sincere appreciation also extends to all my friends who have lend their hands throughout my study. Their views and suggestions are helpful indeed.

Last but not least, I would like to thank my parents and my younger brother for their encouragement, helping me to stay determined while overcoming the challenges ahead.

ABSTRACT

The purpose of this research is to design an enhanced human knee cartilage evaluation framework to detect cartilage thinning in the early Osteoarthritis (OA) disease. The existing research drawbacks include the absence of contrast enhancement model merely on region of interest, the low efficiency and tedious labelling processes in interactive segmentation model, and the lacking of a quantitative assessment in the segmentation model. In this research, we propose a quantitative assessment framework which consists of three phases: Phase 1 focuses on developing an explicit contrast enhancement model for knee images; Phase 2 focuses on developing a reduced interactive cartilage segmentation tool; Phase 3 focuses on formulating a cartilage quantitative measurement. The knee images tested in this research are provided by Osteoarthritis Initiative, given that the sample sizes used were 120, 30 and 20 slices in Phase 1, Phase 2 and Phase 3, respectively. The proposed Prominent Region of Interest Contrast Enhancement (PROICE) method outperformed in diverging the dynamic range of intensity distributed by the region of interest, resulting in noticeable distinctiveness between cartilages and unwanted background tissues. Compared with other existing enhancement methods, PROICE achieved the highest peak signal-to-noise ratio score of 23.80 ± 1.16dB, structural similarity index of 0.86 ± 0.02, low absolute mean error score of 3.88 ± 2.92, and adequate enhancement measure of 17.47 ± 0.74. It was then extended to Enhanced Approximate Non-Cartilage Labels (EANCAL) for the extraction of portions that contained critical information through an entropy filter. This research contributed to reduce human attention level in manual annotations, eventually increased the segmentation efficiency. The modified segmentation framework showed a significant reduction in the mean processing time to 45 ± 4s, which was averaged of 80.25% and 82.25% shorter than manual segmentation for healthy knee cartilage segmentation and diseased knee cartilage segmentation respectively, that performed by two trained operators. In addition, EANCAL obtained an adequate inter-operator reliability score in healthy femoral cartilage (FC) and tibial cartilage (TC) $(FC: 0.920 \pm 0.046; TC: 0.912 \pm 0.044)$. Meanwhile, EANCAL remained competitive compared to the ANCAL method yet with fewer human attention level required, recorded with the highest intra-operator reproducibility score of 0.820 ± 0.074 for operator 1; and 0.833 ± 0.056 for operator 2. The cartilage segmentations were then evaluated with Regional Cartilage Normal thickness approximation (RCN-ta). The quantitative assessment model was validated with FDA-cleared DICOM software, revealed an acceptable error range of $0.135 - 0.214$ mm. The inter-class correlation score and Pearson correlation obtained were $ICC > 0.94$ and $r > 0.90$, respectively. In a nutshell, the PROICE-enhanced images successfully overcome the background seed allocation issue and improved the segmentation model efficiency and segmentation reproducibility, thus yielding a promising cartilage quantitative assessment framework, which potentially assist the clinicians in diagnosis and treatment decision-making process.

ABSTRAK

Tujuan penyelidikan ini adalah untuk merancang penilaian tulang rawan lutut manusia untuk membolehkan pengesanan penipisan osteoartritis lutut awal (OA). Masalah-masalah yang telah dihadapi dalam bidang penyelidikan merangkumi ketiadaan model peningkatan kontras gambar yang menitikberatkan kawasan minat, kecekapan model yang rendah di samping dengan proses pelabelan yang bosan, dan kekurangan perumusan ukuran kuantitatif dalam model segmentasi. Dalam penyelidikan ini, kami mencadangkan kerangka penilaian kuantitatif yang terdiri daripada tiga fasa: Fasa 1 berfokus pada pengembangan model peningkatan kontras eksplisit untuk gambar lutut; Fasa 2 memfokuskan pada pengembangan alat segmentasi tulang rawan interaktif yang ditambahbaikan; Fasa 3 menumpukan pada merumuskan pengukuran kuantitatif tulang rawan. Gambar lutut yang diuji dalam penyelidikan ini dibekalkan oleh badan Osteoarthritis Initiative. Saiz sampel yang digunakan adalah 120, 30 dan 20 keping bagi Fasa 1, Fasa 2 dan Fasa 3. Kaedah penambahbaikan kawasan minat yang dicadangkan (PROICE) mengungguli jurang intensiti dinamik yang disebarkan oleh wilayah tertentu untuk menghasilkan perbezaan yang jelas antara tulang rawan dan tisu latar belakang. Berbanding dengan peningkatan lain yang ada, PROICE mencapai skor *peak signal-to-noise ratio* tertinggi 23.80 ± 1.16 dB, indeks kesamaan struktur 0.86 ± 0.02, skor ralat min mutlak rendah 3.88 ± 2.92 dan ukuran peningkatan yang mencukupi 17.47 ± 0.74. PROICE diperluaskan ke EANCAL yang membolehkan pengekstrakan bahagian yang mengandungi maklumat tinggi dengan saringan entropi. Penyelidikan ini menyumbang dalam mengurangkan tahap perhatian manusia dalam anotasi manual, akhirnya meningkatkan kecekapan segmentasi. Kerangka segmentasi yang ditambahbaikan menunjukkan penurunan yang signifikan pada masa pemprosesan min sebanyak 80.25% dan 82.25% dari segmentasi manual untuk segmentasi tulang rawan lutut yang sihat dan segmentasi tulang rawan lutut penyakit berbanding dengan segmentasi manual selama $45 \pm 4s$, seperti yang dicatat oleh pemerhati 1 dan pemerhati 2. Di samping itu, EANCAL memperoleh skor kebolehpercayaan antara pemerhati yang mencukupi pada tulang rawan femoral yang sihat (FC) dan tulang rawan tibial (TC) (FC: 0.920 ± 0.046; TC: 0.912 ± 0.044). Sementara itu, EANCAL tetap berdaya saing dengan kaedah ANCAL namun dengan tahap perhatian manusia yang kurang, mencatatkan skor kebolehulangan intra-pemerhati yang tertinggi 0.820 ± 0.074 untuk pemerhati 1; dan 0.833 ± 0.056 untuk pemerhati 2. Segmentasi tulang rawan dinilai dengan pendekatan ketebalan normal tulang rawan (RCN-ta). Model penilaian kuantitatif disahkan dengan perisian DICOM yang diiktirafkan oleh FDA, mencatatkan julat ralat yang 0.135-0.214 mm. Skor korelasi antara kelas dan korelasi Pearson yang diperoleh adalah $ICC > 0.94$ dan $r > 0.90$. Ringkasnya, gambar yang disempurnakan dengan PROICE berjaya mengatasi masalah peruntukan benih latar belakang dan meningkatkan kecekapan model segmentasi, di samping dengan kebolehulangan segmentasi, menghasilkan kerangka penilaian kuantitatif tulang rawan yang baik dan berpotensi membantu doktor dalam proses membuat keputusan diagnosis dan rawatan.

TABLE OF CONTENTS

LIST OF TABLES

LIST OF FIGURES

LIST OF ABBREVIATIONS

2D	-	Two dimensional
2DHE	-	Two-Dimensional Histogram Equalization
3D	-	Three dimensional
ACM	-	Active Contour Model
AGCWD	-	Adaptive Gamma Correction with Weighted Distribution
AHE	-	Adaptive Histogram Equalization
AID	-	Absolute Intensity Difference
AMBE	-	Absolute Mean Brightness Error
ANCAL	-	Approximate Non-Cartilage Labels
ASACM	-	Adaptive-Scale Active Contour Model
ASM	-	Active Shape Model
BBCCE	-	Bi-Bezier Curve Contrast Enhancement
BBHE	-	Brightness Preserving Bi-Histogram Equalization
BN	-	Batch Normalisation
BRISQUE	-	Blind or Reference-less Image Spatial Quality Evaluator
CDF	-	Cumulative Density Function
CE	-	Contrast Enhancement
CED	-	Convolutional Encoder-Decoder
CEDHE	-	Contrast Enhancement Dynamic Histogram Equalization
CLAHE	-	Contrast Limited Adaptive Histogram Equalization
CNN	-	Convolutional Neural Network
CT	-	Computed Tomography
DESS	-	Dual-Echo Steady-State
DL	-	Deep Learning
DSIHE	-	Dualistic Sub Image Histogram Equalization
EANCAL	-	Enhanced Approximate Non-Cartilage Labels
ECM	-	Extracellular Matrix
EDT	-	Euclidean Distance Transformation
EME	-	Measure of Enhancement
FC	-	Femoral Cartilage

FCM	-	Fuzzy c-means
FDA	-	Food and Drug Administration
FL	-	Field Line
FN	-	False Negative
FOV	-	Field of View
FP	-	False Positive
FR	-	Full Reference
GAG	-	Glycosaminoglycan
GC	-	Graph Cut
GCAELEWD	-	Gamma Correction Adaptive Extreme-Level Eliminating with Weighting Distribution
GHE	-	General Histogram Equalization
GLCM	-	Gray Level Co-occurrence Matrix
GMM	-	Gaussian Mixture Model
GRE	-	Gradient-Recalled Echo
GVF	-	Gradient Vector Flow
GVFOM	-	Gradient Vector Flow Over Manifold
HE	-	Histogram Equalization
IDV	-	Intensity Discrepancy Value
IQA	-	Image Quality Assessments
JSN	-	Joint-Space Narrowing
JSW	-	Joint-Space Width
KH	-	Krill Herd
KL	-	Kellgren-Lawrence
K-NN	-	K-Nearest Neighbours
LACS	-	Local-Area Cartilage Segmentation
LOGISMOS	-	Layered Optimal Graph Image Segmentation of Multiple Objects and Surfaces
LSD	-	Least Significant Difference
LSH	-	Locally-Sensitivity Hashing
LWV	-	Locally Weighted Vote
MCC	-	Matthew’s Correlation Coefficient
MedGA	-	Medical imaging Enhancement with Genetic Algorithm

mJSW	-	Minimum Joint-Space Width
MMBEBHE	-	Minimum Brightness Error Bi-Histogram Equalization
MRI	-	Magnetic Resonance Imaging
MSCN	-	Mean Substracted Contrast Normalization
MSE	-	Mean Squares of Errors
MSG	-	Moth Swarm Algorithm
NIQE	-	Naturalness Image Quality Evaluator
NPHE	-	Non-Parametric Modified Histogram Equalization
NR	-	No Reference
NROI	-	Non-Region of Interest
NSAIDS	-	Non-Steroidal Anti-Inflammatory Drugs
NSS	-	Natural Scene Statistics
OA	-	Osteoarthritis
OAI	-	Osteoarthritis Initiative
PCA	-	Principal Component Analysis
PCR	-	Pixel Concentration Rate
PDF	-	Probability Density Function
PROICE	-	Prominent Region of Interest Contrast Enhancement
PSNR	-	Peak Signal-to-Noise Ratio
RCN-ta	-	Regional Cartilage Normal thickness approximation
RDHACEM	-	Reversible Data Hiding with Automatic Contrast Enhancement
ReLU	-	Rectified Linear Unit
RMSE	-	Root Mean Square Error
RMSHE	-	Recursive Mean Separate Histogram Equalization
ROI	-	Region of Interest
RW	-	Random Walker
SE	-	Spin-Echo
Sens	-	Sensitivity
SF	-	Synovial Fluid
Spec	-	Specificity
SSGCM	-	Spatial Stimuli Gradient Sketch Model
SSIM	-	Structural Similarity Index

SSM	-	Statistical Shape Model
SVM	-	Support Vector Machine
TBCSSR	-	Tuned Brightness Controlled Single-Scale Retinex
TC		Tibial Cartilage
TN	-	True Negative
TP	-	True Positive
TSSR	-	Tuned Single-Scale Retinex Algorithm
US	-	Ultrasonographic
VASc	-	Visual Analog Scales
we	-	Water Excitation
ICC	-	Intra-class Correlation

LIST OF SYMBOLS

CP_{lower}	-	Lower Control Points
CP_{upper}	-	Upper Control Points
L_{ij}	-	Combinatorial Laplacian Matrix
$P_{Global\ maximum}$	-	Global Maximum Points
$P_{Global\ minimum}$	-	Global Minimum Points
P_{avg}	-	Average Pixel Distance
T_{bp}	-	Bimodal Distribution Threshold Value
b_j	-	Cartilage or Non-cartilage Label
cdf_{lower}	-	Lower Cumulative Density Function
cdf_{upper}	-	Upper Cumulative Density Function
d_l	-	Luminance Difference
d_s	-	Spatial Difference
f_c	-	Cost Function
f_{lower}	-	Lower Transformation
f_{upper}	-	Upper Transformation
AID	-	Absolute Intensity Difference
B	-	Bernstein Polynomials
D	-	Degree Matrix
$D[.]$	-	Combinatorial Dirichlet
G	-	Gaussian Filter
H	-	Entropy filter
Ind	-	Cartilage Indicator
L	-	Maximum Intensity Level
N	-	Gaussian Mixture
O	-	Orientation of Selection Cartilage Boundary
P	-	Probability Distribution
Q	-	Bezier Curve
$Q(M)$	-	Ranking function
c	-	Intersection Point in Linear Equation

cdf	-	Cumulative Density Function
g	-	Gradient operator
pdf	-	Probability Density Function
sp	-	Superpixel Centre
w	-	Weight
μ	-	Mean of pixel value
σ	-	Standard Deviation
ϑ	-	EANCAL Cost Function Constant

LIST OF APPENDICES

CHAPTER 1

INTRODUCTION

1.1 Introduction to Osteoarthritis

Osteoarthritis (OA) is a major public health issue globally. OA is the most seen arthritis and cause of disability. Barbour, Helmick, Boring and Brady (2017) stated that about 54.4 million adults in the US had arthritis after diagnosed by doctors which was a huge leap from 46 million patients recorded in 2003 (Rosenfeld, 2010). Meanwhile, 10% to 20% of the elderly population were estimated to have OA. According to the COPCORD survey, knee pain is one of the most received rheumatic complaints in Malaysia, with 64.8% of joint complaints while more than half were diagnosed to have clinical symptoms (Veerapen, Wigley and Valkenburg, 2007).

OA is a type of arthritis that is caused by gradual loss of cartilage for one or more joints. It could be categorised clinically by its pain, enlargement, deformation of cartilage, and limitation of motion (Dunlop *et al.*, 2003), which normally influences the elderly. The risk factors are obesity, elevated BMI, and aging problem (Rosenfeld, 2010). However, Wallace *et al.* (2017) mentioned that these factors were insufficient to reason the exponential growth in prevalence of knee OA. These authors hypothesised that the decrement in physical activity could be one of the contributing factors. The underloaded joints with lower protein glycan content and weaker muscles could fail to stabilise the joints at their positions. On the contrary, another study showed that both T1 rho and T2 mapping sequences could reflect the impact that caused by different physiological activities on knee cartilage. He reasoned that fluid shifts, collagen fibre deformation, spatial heterogeneity, tissue stiffness, and differences in material characteristics have a close relationship with cartilage loading properties (Chen *et al.*, 2017).

The fully worn knee articular cartilage is irreversible and could bring great pain to the patients. Patients, especially aging women, prone to be affected by OA and gradually endure cartilage loss without any apparent symptoms at the early stage. As the condition worsens, the cartilages become thinner and some parts of the bone that are responsible (Bijlsma, Berenbaum and Lafeber, 2011) to protect underneath the cartilage starts to get exposed. Some patients tried to get medication after experiencing severe knee pain and realising the disease, but it was often too late as the cartilage has been fully damaged or late disease stage. The collision between femur and tibia bones could result in unbearable pain that forces the patients to rely on pain-relieving drugs. Eventually, chronic OA patients will suffer from loss of mobility and function which severely degrades their daily life (Brooks, 2002). However, early OA can be detected at an early stage through radiography and MR imaging, thus the early therapies can inhibit the disease progression (Befrui *et al.*, 2018).

Meanwhile, there are several treatments available for the disease, including non-pharmacological treatment, pharmacological treatment, and hyaluronic acid injection. For weight-bearing joints, the non-pharmacological method, for instance, losing weight, exercise (Christensen, Bartels, Astrup and Bliddal, 2007) and physical therapy are more concerned (Deyle *et al.*, 2000). To reduce the pain and knee joint inflammation, patients will obtain medication from their doctors (Lawson *et al.*, 2004). The pharmacological treatments aim to reduce knee inflammation while reducing the pain with Non-Steroidal Anti-Inflammatory Drugs (NSAIDS) in combination with other existing medications such as proton pump inhibitors (Steinmeyer *et al.*, 2018). Some patients might receive hyaluronic acid injection to keep the tissues moist and well lubricated. To permanently overcome the knee pain, some patients will choose to undergo knee cartilage replacement surgery to have their cartilage replaced with artificial cartilage (Bachmeier *et al.*, 2001).

1.2 Background of Research

Instead of 2D radiography and ultrasonography, magnetic resonance imaging (MRI) shows robustness in detecting lesions and monitoring the pharmacological effect or therapeutic effect (Schaefer *et al.*, 2017). From a safety perspective, radiography technologies expose the patients to radiation and can cause a long-term health hazard. The 2D radiography and ultrasonography hinder an overall assessment of the knee cartilage defects, while MRI allows visualisation for a complete structure of knee cartilage non-invasively (González and Escalante-Ramírez, 2013). The available sequences (Crema *et al.,* 2011) for the MRI in viewing knee anatomy are standard spin-echo (SE) and gradient-recalled echo (GRE), fast SE, three-dimensional SE and GRE. MRI definition of OA contains more features compared to the 2D radiographic definition, hence it is more sensitive towards detection of early OA with a more valid definition than 2D radiography (Schiphof *et al.*, 2014).

MRI scans are often contaminated with noises, unwanted artifacts and poor background illuminance (Teh *et al.*, 2018; Gan, Swee, *et al.*, 2014). Moreover, the human knee is one of the most anatomically complex parts of the human body. Excellent contrast enhancement is vital to overcome the issues, for instance, indistinct tissue contrast and low-brightness appearance, to boost the visual perception of Region of Interest (ROI) in knee MR images (Gandhamal *et al.*, 2017).

However, most of the existing contrast enhancement methods fail to retain the important information in the medical images. Conventional histogram equalization brightens the medical images globally (Huang *et al.*, 2013) that distorted the overall image quality. Later, there were more mean or median preserving and sub-histogram separation contrast improvement methods (Kim, 1997; Park, Cho and Choi, 2008) being proposed to overcome the drawbacks of the conventional method. Nonetheless, these commonly-used methods were not designed explicitly for medical imaging purposes and could potentially wash out the boundaries (Gan *et al.,* 2014). Thus, unsuitable methods could increase the difficulty in identifying the cartilages from other knee soft tissues and synovial fluid.

Meanwhile, the recently proposed methods in enhancing medical images, such as Gamma Correction Adaptive Extreme-Level Eliminating with Weighting Distribution (Teh *et al.*, 2018), Reversible Data Hiding method (Gao *et al.*, 2021), novel krill herd-based method (Kandhway *et al.*, 2020), multi-modal medical image fusion-based method (Maqsood and Javed, 2020) and Bi-Bezier Curve enhancement method (Gan, Swee, *et al.*, 2014), show greater relevancy in contributing adequate improvement to lift the medical images' brightness gently while maintaining the structural features.

The procedure is normally followed by the segmentation stage that has a significant influence on the accuracy of cartilage quantitative assessment in the following stage (Faisal *et al.*, 2018). In recent years, knee cartilage segmentation models that have been developed are mostly manual segmentation model, semi-automatic segmentation model and automatic segmentation model. As the morphological changes in the knee occur at a very slow rate, the segmentation methods required must be highly reproducible (Eckstein *et al.*, 2006). As the cartilage exhibited huge anatomical variation, thin, irregular cartilage structure and pathological characteristics, the models demand expert supervision and validation. However, human experts may make a different conclusion regarding the severity and presence of the disease, therefore it requires knowledge and experience to make a valid OA diagnosis (Mahapatra, 2013). Moreover, the manual knee cartilage segmentation is conducted by a trained operator which can take a few hours to segment a single whole knee (Fripp *et al.*, 2010).

Several studies have been added these years on developing fully automatic knee segmentation models by training the deep learning convolutional neural network (Su *et al.*, 2017; Liu *et al.*, 2018). However, the segmentation with promising accuracy requires a substantial amount of labelled data, training data and validation data (Liu *et al.*, 2018). Therefore, interactive segmentation model becomes an alternative that involves human intervention in providing crucial information of the image to the computer, then the computer will replace the manual delineation to conduct the segmentation (Kim *et al.*, 2020; Yin *et al.*, 2010).

During normal aging, 0.3% to 0.5% of cartilage lost per year is estimated and can be hardly detected (Gray *et al.*, 2004). Clinical trials for osteoarthritis therapy highly rely on structural change (Schaefer *et al.*, 2017) to identify the statistically significant transformation in disease progression of degeneration or durability of repair tissue. Morphological imaging biomarker in identifying the cartilage thickness is critically important to detect the early OA. However, the cartilage thickness is computed with topography (Rogowska *et al.*, 2003) and measured by a hand-held ultrasonic probe where the measurement accuracy can be adversely affected by several control factors (Steppacher *et al.*, 2019; Schmitz *et al.*, 2017).

As MRI benefits in offering full knee visualisation as compared to other radiography methods, there are 3-dimensional cartilage volume quantitative assessments (Schaefer *et al.*, 2017; Kauffmann *et al.*, 2003) being proposed to allow longitudinal disease follow-ups. However, the volume assessment models demand strict validation with synthetic model or water displacement method with disarticulated cartilages.

1.3 Problem Statement

The central problem of the existing studies is the lack of focused study on identifying the non-cartilage labels (knee bones, fat pad, muscles, ligaments and nearby fluids). The pathological changes in knee cartilage are inconsistent thus bringing down the available segmentation methods in extracting the cartilaginous portion. Several studies also suggested to conduct pre-segmentation or registration to a more rigid bone structure prior to apply the deformable models onto the cartilages (Fripp *et al.*, 2010; Yin *et al.*, 2010; Wang *et al.*, 2016). A non-cartilage labels approximation model was proposed to allocate the background seeds automatically (Gan *et al.*, 2014) to efficiently reduce the labelling work that required intensive expert supervision. As a basis of this study, the researcher defined the overall problem of the non-cartilage labels approximation model to be threefold.

Problem 1: Failure in background seed placement, typically in bone regions and synovial cavity.

The automated background seed placement model mimics the human visual system (Gan *et al.*, 2014). Generally, the ROI shall result in a higher quantification level. However, the low-contrast nature in knee MRIs causes ambiguity in the quantification stage. The regions of high homogeneity with cartilages would be mis-quantified at high level, and hence fail in seed placement in these regions. Therefore, it requires a series of image enhancement techniques to improve the inferior visual appearance not only to help the physicians in abnormality detection and diagnosis decision making processes (Rundo *et al.*, 2019) but also to improve the segmentation (Desai and Hacihaliloglu, 2019; Kandhway *et al.*, 2020) or classification accuracy rate in the following stage. The biggest concern in knee image is the indistinctiveness between the cartilage and the connecting regions. However, the improvement in tissue distinctiveness was not focused in these studies.

Problem 2: Interactive input to draw cartilage labels could be tedious and time-consuming if substantial datasets are involved.

The existing interactive segmentation models require heavy attention from the operator and prior knowledge to conduct image registration and shape model allocation. As such, the researchers raised the concern in reducing the human attention level in the labelling stage (Gan *et al.*, 2014). Nonetheless, the existing interactive segmentation models require extensive user input in allocating the labels (Gan *et al.*, 2014) or multi-atlas registration (Lee *et al.*, 2016) by human operator. The laborious processes could be tedious when enormous datasets are examined. Therefore, the segmentation model demands a reduction in terms of user inputs to improve the efficiency of the model while securing a good segmentation accuracy.

Problem 3: Lack of a knee quantitative assessment in the knee MRI segmentation model.

The direct thickness computations on MRI cartilage segmentation slices could detect the thinning region of both femoral and tibial cartilages. Most of the direct measurements are conducted through A-mode ultrasound (Steppacher *et al.*, 2019), cartilage thickness (Desai and Hacihaliloglu, 2019; Faisal *et al.*, 2018) from ultrasounds, and joint space measurements (Cao *et al.*, 2015). However, the normal cartilage thickness evaluation model for segmented cartilage is found lacking in the past studies.

1.4 Research Objectives

Given the absence of promising and effective treatments available in late OA disease, signalling the demand for a knee cartilage evaluation model in detecting early cartilage thinning. The framework of the proposed model includes the solutions to overcome the stated problems. Several objectives have been identified as follows:

1. To propose a prominent region of interest contrast enhancement technique to enhance the articular cartilage contrast to become more distinctive from other soft tissues and synovial fluid.

2. To formulate a minimal interactive enhanced approximate non-cartilage labels model to extract knee tibiofemoral cartilages from the knee MR images.

3. To propose a regional cartilage thickness approximation technique to compute human knee cartilage thickness in normal distance between bone surface and cartilage layer.

1.5 Research Scope

The research was conducted in three phases: Phase 1 to enhance the knee MRI; Phase 2 involved background labels approximation and interactive segmentation stage to yield tibiofemoral cartilages; Phase 3 involved knee cartilage quantitative assessment. Details of the research scope were stated as follow:

1. Use of only dual-echo steady-state (DESS) with water excitation (we) MR image of human knee cartilage provided by Osteoarthritis Initiative (OAI). All the OAI DESSwe MR images used in the study were in sagittal view and captured under magnetic strength of 3 Tesla. The image packages include the images of participants from baseline datasets.

2. Classification of MR image into healthy and diseased classes referring to Kellgren-Lawrence grades, as shown in Table 1.1. The classified images underwent a second-time classification by two experienced radiologists.

Table 1.1 Kellgren-Lawrence grading system for OA disease. (Kellgren and Lawrence, 1957)

Grade	**Descriptions**
0	No radiological findings of osteoarthritis
1	Doubtful narrowing of joint space and possible osteophytic lipping
2	Definite osteophytes and possible narrowing of joint space
3	Moderate multiple osteophytes, define narrowing of joint space, small pseudocystic areas with sclerotic walls and possible deformity of bone contour
4	Large osteophytes, marked narrowing of joint space, severe sclerosis and definite deformity of bone contour

3. Age of participants ranges from 45 to 79 years old. Major exclusion criteria include inflammatory arthritis, bilateral end-stage knee OA, and contraindication to 3T MRI. The sample sizes used in this research are tabulated in Table 1.2.

Table 1.2 Sample sizes for validating the models in three phases.

Phase	Male	Female	Total Sample Size
1	38	82	120
2	12	18	30
3	9	11	20

4. MATLAB 2019a was used to develop the algorithms for all the image processing procedures introduced in the study. SPSS was utilized to analyse the data.

5. The most affected region, specifically the medial compartment of the knee was referred to in the study, referring to Figure 1.1. The medial compartment supports $60 - 80\%$ of the weight-bearing load while experiencing normal ambulation in healthy knees (Vincent *et al.*, 2013).

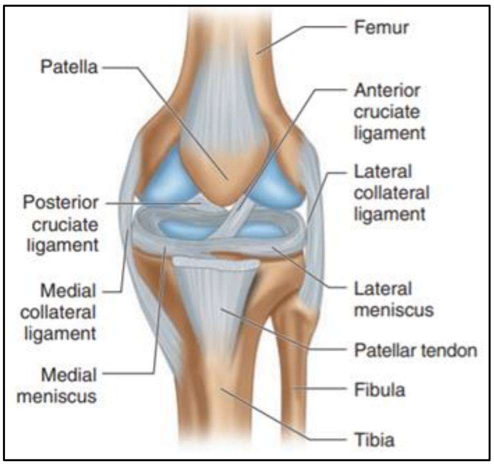

Figure 1.1 Human knee anatomy. (Gold *et al.*, 2019)

6. Knee cartilage segmentations were performed in 2-dimensions (2D). 3-dimensions (3D) reconstructions of cartilages were not included in the proposed study due to the lack of a validation model, such as the synthetic knee model (Kauffmann *et al.*, 2003) or disarticulated cartilage (Millington *et al.*, 2007; Graichen *et al.*, 2003).

7. This research does not consider the advanced clinical longitudinal follow-ups in tracking the disease progression.

1.6 Significance of Research

The proposed research focused on developing a complete OA disease progression evaluation framework, starting from knee image enhancement, computer-aided segmentation network and finally cartilage thickness computation.

Most of the existing contrast enhancement methods aim to have full contrast stretching which influences the overall brightness and the crucial details. The proposed contrast enhancement method focused on strengthening the sub-distribution exhibited by the ROI. The regions with homogenous intensities and texture characteristics, such as fat, synovial fluid and muscles, would be further diverged and causes the cartilage texture to be different from the other portions. The contrast enhancement model contributed to reduce the ambiguity in identifying the cartilaginous pixels and potentially assist the physicians in decision making and disease diagnosis.

Moreover, a highly reproducible interactive segmentation model can greatly reduce the time required by manual segmentation which normally takes several hours. The previous Approximate Non-Cartilage Labels required manual labelling in cartilage annotations. Furthermore, the model often failed in placing adequate background seed due to pre-set threshold value of 100. The enhanced model replaced the manual label delineation with more user-friendly inputs and resolved the seed placement issue with an improved quantification technique and an automated threshold estimation mechanism.

The medial tibiofemoral cartilages are the most affected area in OA. Therefore, the femoral cartilage and tibial cartilage segmented from the previous stage were further analysed morphologically through normal thickness computation. Utilising linear equations on the Cartesian plane, the normal lines were emitted from one side of the cartilage surface to intersect with the edge points of the opposing side. The average cartilage thicknesses were computed at three weight-bearing regions at each cartilage and the accuracy of the evaluation model was validated with FDA-cleared ONIS DICOM software.

1.7 Thesis Organisation

This thesis introduces an improved semi-automated knee cartilage segmentation model and added with the cartilage thickness computation capability. The total chapters included in this thesis are six chapters.

Chapter 1 introduces the general overview of the study, generates research objectives according to the found problem statements and identifies the research scope that defines the study's boundary. At the end of the chapter, the significances of the proposed study are elaborated.

Chapter 2 reviews the existing contrast enhancement algorithms, cartilage segmentation methods and cartilage quantitative assessments. Through the review, the conceptual development, the strength and weakness of relevant methods are discussed.

Chapter 3 describes the proposed evaluation model methodology. The chapter also includes the development of the ROI sub-distribution contrast enhancement method.

Chapter 4 includes two sections. The first section describes the development of a minimal interactive segmentation model in extracting the cartilages from the knee MR images. Meanwhile, the second section illustrates the design on normal thickness computation from the segmentation result.

Chapter 5 presents the results and discussions about the overall performance of the proposed framework. In the first section, the proposed contrast enhancement method is compared with other existing methods, including both commonly-used methods and medical purpose contrast enhancement methods. In the second section, the Matthew Correlation Coefficient, Dice's coefficient, sensitivity and specificity of the segmentation model are evaluated. Later, the designed cartilage quantitative assessment is validated with ONIS software and the overall performance of the framework is studied.

Chapter 6 concludes the contributions of the proposed study and suggests meaningful recommendations on improving the cartilage evaluation model for future work.

REFERENCES

Ababneh, S.Y., Prescott, J.W. and Gurcan, M.N. Automatic graph-cut based segmentation of bones from knee magnetic resonance images for osteoarthritis research. *Medical Image Analysis*. 2011. 15(4):438–448.

Adams, R., and Bischof, L. Seeded Region Growing. *IEEE Transactions on Pattern Analysis and Machine Intelligence*. 1994. 16(6):641–647.

Agaian S.S., Panetta K. and Grigoryan M. A New Measure of Image Enhancement. *IASTED International Conference on Signal Processing \& Communication*. September 19-22, 2000. Malaga, Spain: ACTA press. 2000. 19–22.

Al-Ameen, Z. Expeditious contrast enhancement for grayscale images using a new swift algorithm. *Statistics, Optimization and Information Computing*. 2018. 6(4):577–587.

Al-Ameen, Z. and Sulong, G. A new algorithm for improving the low contrast of computed tomography images using tuned brightness controlled single-scale Retinex. *Scanning*. 2015. 37(2):116–125.

Al-Ameen, Z. and Sulong, G. Ameliorating the Dynamic Range of Magnetic Resonance Images Using a Tuned Single-Scale Retinex Algorithm. *International Journal of Signal Processing, Image Processing and Pattern Recognition*. 2016. 9(7):285–292.

Alom, M.Z., Taha, M.T., Yakopcic, C., Westberg, S., Sidike, P., Nasrin, M.S., Esesn, B.C., Awwal, A.S.S. and Asari, V.K. The History Began from AlexNet: A Comprehensive Survey on Deep Learning Approaches. *arXiv*. 2018. 1408.3264.

Ambellan, F., Tack, A., Ehlke, M. and Zachow, S. Automated segmentation of knee bone and cartilage combining statistical shape knowledge and convolutional neural networks: Data from the Osteoarthritis Initiative. *Medical Image Analysis*. 2019. 52:109–118.

Asghar, K., Gilanie, G., Saddique, M. and Habib, Z. Automatic enhancement of digital images using cubic Bézier curve and Fourier transformation. *Malaysian Journal of Computer Science*. 2017. 30(4):300–310.

Atkinson, A.J., Colburn, W.A., DeGruttola, V.G., DeMets, D.L., Downing, G.J., Hoth, D.F., Oates, J.A., Peck, C.C., Schooley, R.T., Spilker, B.A., Woodcock, J. and Zeger, S.L. Biomarkers and surrogate endpoints: Preferred definitions and conceptual framework. *Clinical Pharmacology and Therapeutics*. 2001. 69(3):89–95.

Bachmeier, C.J.M., March, L.M., Cross, M.J., Lapsley, H.M., Tribe, K.L., Courtenay, B.G. and Brooks, P.M. A comparison of outcomes in osteoarthritis patients undergoing total hip and knee replacement surgery. *Osteoarthritis and Cartilage*. 2001. 9(2):137–146.

Barbour, K.E., Helmick, C.G., Boring, M. and Brady, T.J. Vital signs: prevalence of doctor-diagnosed arthritis and arthritis-attributable activity limitation—United States, 2013–2015. *MMWR. Morbidity and mortality weekly report*. 2017. 66(9):246.

Befrui, N., Elsner, J., Flesser, A., Huvanandana, J., Jarrousse, O, Le, T.N., Müller, M., Schulze, W.H.W, Taing, S. and Weidert, S. Vibroarthrography for early detection of knee osteoarthritis using normalized frequency features. *Medical and Biological Engineering and Computing*.2 2018. 56(8):1499–1514.

Biggs, N. Algebraic potential theory on graphs. *Bulletin of the London Mathematical Society*. 1997. 29(6):641–682.

Bijlsma, J.W.J., Berenbaum, F. and Lafeber, F.P.J.G. Osteoarthritis: An update with relevance for clinical practice. *The Lancet*. 2011. 377(9783):2115–2126.

Boykov, Y. and Funka-Lea, G. Graph cuts and efficient N-D image segmentation. *International Journal of Computer Vision*. 2006. 70(2):109–131.

Boykov, Y. and Kolmogorov, V. An experimental comparison of min-cut/max-flow algorithms for energy minimization in vision. *Lecture Notes in Computer Science (including subseries Lecture Notes in Artificial Intelligence and Lecture Notes in Bioinformatics)*. 2001. 2134(9):359–374.

Brem, M.H.. Lang, P.K., Neumann, G., Schlechtweg, P.M., Schneider, E., Jackson, R. Yu, J., Eaton, C.B., Hennig, F.F., Yoshioka, H. Pappas, G. and Duryea J. Magnetic resonance image segmentation using semi-automated software for quantification of knee articular cartilage - Initial evaluation of a technique for paired scans. *Skeletal Radiology*. 2009. 38(5):505–511.

Brooks, P.M. Impact of osteoarthritis on individuals and society: How much disability? Social consequences and health economic implications. *Current Opinion in Rheumatology*. 2002. 14(5):573–577.

Buckland-Wright, J.C., Macfarlane, D.G., Williams, S.A. and Ward, R.J. Accuracy and precision of joint space width measurements in standard and macroradiographs of osteoarthritic knees. *Annals of the Rheumatic Diseases*. 1995. 54(11):872–880.

Bui, T., Ahn, C., Shin, J. and Lee, Y.W. Fully automatic segmentation based on localizing active contour method. *Proceedings of the 8th International Conference on Ubiquitous Information Management and Communication, ICUIMC 2014*. New York: 2014 ACM Press. 2014.1–5.

Cabezas, M., Oliver, A., Lladó, X., Freixenet, J. and Cuadra, M.B. A review of atlas-based segmentation for magnetic resonance brain images. *Computer Methods and Programs in Biomedicine*. 2011. 104(3):.e158–e177.

Cai, Q., Liu, H., Zhou, S., Sun, J. and Li, J. An adaptive-scale active contour model for inhomogeneous image segmentation and bias field estimation. *Pattern Recognition*. 2018. 82:79–93.

Canny, J. A computational approach to edge detection. *IEEE Transactions on pattern analysis and machine intelligence*. 1986. 1986(6):679–698.

Cao, J., Zheng, B., Meng, X., Lv, Y., Lu, H., Wang, K., Huang, D. and Ren, J. A novel ultrasound scanning approach for evaluating femoral cartilage defects of the knee: comparison with routine magnetic resonance imaging. *Journal of Orthopaedic Surgery and Research*. 2018. 13(1):178.

Cao, Q., Thawait, G., Gang, G.J., Zbijewski, W., Reigel, T., Brown, T., Corner, B., Demehri, S. and Siewerdsen, J.H. Characterization of 3D joint space morphology using an electrostatic model (with application to osteoarthritis). *Physics in Medicine and Biology*. 2015. 60(3): 947–960.

Carballido-Gamio, J. and Majumdar, S. Atlas-based knee cartilage assessment. *Magnetic Resonance in Medicine*. 2011. 66(2):575–581.

Celik, T. Two-dimensional histogram equalization and contrast enhancement. *Pattern Recognition*. 2012. 45(10):3810–3824.

Chan, T.F., Yezrielev Sandberg, B. and Vese, L.A. Active contours without edges for vector-valued images. *Journal of Visual Communication and Image Representation.* 2000. 11(2):130–141.

Chen, M., Qiu, L., Shen, Si., Wang, F., Zhang, J. and Liu, Si. The influences of walking, running and stair activity on knee articular cartilage: Quantitative MRI using T1 rho and T2 mapping. *PLoS ONE*. 2017. 12(11):e0187008.

Chen, S. Der and Ramli, A.R. Contrast enhancement using recursive mean-separate histogram equalization for scalable brightness preservation. *IEEE Transactions on Consumer Electronics*. 2003a. 49(4):1301–1309.

Chen, S. Der and Ramli, A.R. Minimum mean brightness error bi-histogram equalization in contrast enhancement. *IEEE Transactions on Consumer Electronics*. 2003b. 49(4):1310–1319.

Chen, X. and Pan, L. A Survey of Graph Cuts/Graph Search Based Medical Image Segmentation. *IEEE Reviews in Biomedical Engineering*. 2018. 11:112–124.

Christensen, R., Bartels, E.M., Astrup, A. and Bliddal, H. Effect of weight reduction in obese patients diagnosed with knee osteoarthritis: A systematic review and meta-analysis. *Annals of the Rheumatic Diseases*. 2007. 66(4):433–439.

Cootes, T., Taylor, C., Cooper, D. and Graham, J. Active shape models-their training and application. *Computer Vision and Image Understanding*. 1995. 61(1):38–59.

Cortes, C. and Vapnik, V. Support-vector networks. *Machine Learning*. 1995. 20(3):273–297.

Crema, M.D., Roemer, F.W., Marra, M.D., Burstein, D., Gold, G.E., Eckstein, F., Baum, T., Mosher, T.J., Carrino, J.A. and Guermazi, A. Articular Cartilage in the Knee: Current MR imaging techniques and applications in clinical practice and research. *Radiographics*. 2011. 31(1):37–61.

Desai, P. and Hacihaliloglu, I. Knee-cartilage segmentation and thickness measurement from 2D ultrasound. *Journal of Imaging*. 2019. 5(4):1–19.

Deyle, G.D., Henderson,, N.E., Matekel, R.L., Ryder, M.G., Garber, M.B. and Allison, S.C. Effectiveness of manual physical therapy and exercise in osteoarthritis of the knee: A randomized, controlled trial. *Annals of Internal Medicine*. 2000. 132(3):173–181.

Dijck, C., Wirix-Speetjens, R., Jonkers, I. and Vander Sloten, J. Statistical shape model-based prediction of tibiofemoral cartilage. *Computer Methods in Biomechanics and Biomedical Engineering*. 2018. 21(9):568–578.

Dougherty, G. *Digital Image Processing for Medical Applications*. New York: Cambridge University Press. 2009.

Duarte, A., Hegde, C.V., Kaku, A., Mohan, S. and Raya, J.G. Knee Cartilage Segmentation Using Diffusion-Weighted MRI. 2019. *arXiv*. 1912.01838.

Dunlop, D.D., Manheim, L.M., Yelin, E.H., Song, J. and Chang, R.W. The costs of arthritis. *Arthritis Care and Research*. 2003. 49(1):101–113.

Dunnhofer, M., Antico, M., Sasazawa, F., Takeda, Y., Camps, S., Martinel, N., Micheloni, C., Carneiro, G. and Fontanarosa, D. Siam-U-Net: encoder-decoder siamese network for knee cartilage tracking in ultrasound images. *Medical Image Analysis*. 2020. 60:101631.

Duzenli, T., Ata, E. and Kosem, M. Ultrasonographic Assessment of Knee Cartilage Thickness in Patients with Ulcerative Colitis: Decreased Femoral Cartilage Thickness May Be an Indicator of Extraintestinal Manifestation in Patients with Mild Activity Ulcerative Colitis. *Cartilage*. 2020. 1–7.

Eckstein, F., Collins, J.E., Nevitt, M.C., Lynch, J.A., Kraus, V., Katz, J.N., Losina, E., Wirth, W., Guermazi, A., Roemer, F.W. and Hunter, D.J. Brief Report: Cartilage Thickness Change as an Imaging Biomarker of Knee Osteoarthritis Progression: Data From the Foundation for the National Institutes of Health Osteoarthritis Biomarkers Consortium. *Arthritis & Rheumatology*. 2015. 67(12):3184–3189.

Eckstein, F., Guermazi, A., Gold, G., Duryea, J., Graverand, M.P.H.L., Wirth, W. and Miller, C.G. Imaging of cartilage and bone: Promises and pitfalls in clinical trials of osteoarthritis. *Osteoarthritis and Cartilage*. 2014. 22(10):1516–1532.

Eckstein, F., Cicuttini, F., Raynauld, J.P., Waterton, J.C. and Peterfy, C. Magnetic resonance imaging (MRI) of articular cartilage in knee osteoarthritis (OA): morphological assessment. *Osteoarthritis and Cartilage*. 2006. 14:46–75.

Faisal, A., Ng, S.C., Goh, S.L. and Lai, K.W. Knee cartilage segmentation and thickness computation from ultrasound images. *Medical and Biological Engineering and Computing*. 2018. 56(4):657–669.

Fix, E. and Hodges, J. Nonparametric discrimination: consistency properties. *Randolph Field, Texas (No. 4)*. Project 21-49-004. 1951. 21–49.

Folkesson, J., Dam, E., Olsen, O.F., Pettersen, P. and Christiansen, C. Automatic segmentation of the articular cartilage in knee MRI using a hierarchical multi-class classification scheme. *Lecture Notes in Computer Science (including subseries Lecture Notes in Artificial Intelligence and Lecture Notes in Bioinformatics)*. 2005. 327–334.

Ford, L.R. and Fulkerson, D.R. Maximal flow through a network. *Canadian Journal of Mathematics*. 2018. 70(1):399–404.

Fripp, J., Crozier, S., Warfield, S.K. and Ourselin, S. Automatic segmentation and quantitative analysis of the articular cartilages from magnetic resonance images of the knee. *IEEE Transactions on Medical Imaging*. 2010. 29(1):55–64.

Gan, H.S., Tan, T.S., Wong, L.X., Tham, W.K., Sayuti, K.A., Karim, A.H. A., Kadir, M.R.A. Interactive knee cartilage extraction using efficient segmentation software: Data from the osteoarthritis initiative. *Bio-Medical Materials and Engineering*. 2014. 24(6):3145–3157.

Gan, H.S., Tan, T.S., Karim, A.H.A., Sayuti, K.A. and Kadir, M.R.A. Interactive medical image segmentation with seed precomputation system: Data from the Osteoarthritis Initiative. *IECBES 2014, Conference Proceedings - 2014 IEEE Conference on Biomedical Engineering and Sciences: 'Miri, Where Engineering in Medicine and Biology and Humanity Meet'*. December 8-10, 2014. Miri: IEEE. 2014. 315–318.

Gan, H.S., Tan, T.S., Kadir, M.R.A., Sayuti, K.A., Wong, L.X. and Tham, W.K. Medical image contrast enhancement using spline concept: Data from the osteoarthritis initiative. *Journal of Medical Imaging and Health Informatics*. 2014. 4(4):511–520.

Gan, H.S., Swee, T.T., Karim, A.H.A, Sayuti, K.A., Kadir, M.R.A, Tham, W.K., Wong, L.X., Chaudhary, K.T., Ali, J. and Yupapin, P.P. Medical image visual appearance improvement using bihistogram bezier curve contrast enhancement: Data from the osteoarthritis initiative. *Scientific World Journal*. 2014. 2014(July):1–13.

Gandhamal, A., Talbar, S., Gajre, S., Hani, A.F.M. and Kumar, D. A generalized contrast enhancement approach for knee MR images. *2016 International Conference on Signal and Information Processing, IConSIP 2016*. October 6-8, 2016. Maharashtra. IEEE. 2017. 1–6.

Gao, G., Tong, S., Xia, Z., Wu, B., Xu, L. and Zhao, Z. Reversible data hiding with automatic contrast enhancement for medical images. *Signal Processing*. 2021. 178:107817.

Ghosh, S., Beuf, O., Ries, M., Lane, N.E., Steinbach, L.S. , Link, T.M. and Majumbar, S. Watershed segmentation of high resolution magnetic resonance images of articular cartilage of the knee. *Annual International Conference of the IEEE Engineering in Medicine and Biology - Proceedings*. July 23-28, 2000. Chigago: IEEE. 2000. 4(I):3174–3176.

Glocker, B., Komodakis, N., Paragios, N., Glaser, C., Tziritas, G. and Navab, N.. Primal/dual linear programming and statistical atlases for cartilage segmentation. *Lecture Notes in Computer Science (including subseries Lecture Notes in Artificial Intelligence and Lecture Notes in Bioinformatics)* .2007. 536–543.

Gold, P.A., Jones, M.R. and Kaye, A.D. Knee Joint Pain. *Pain*. 2019. 761–765.

González, G. and Escalante-Ramírez, B. Knee cartilage segmentation using active shape models and contrast enhancement from magnetic resonance images. *IX International Seminar on Medical Information Processing and Analysis*. 2013. 8922:892213.

Gonzalez, R.C., Woods, R.E. and Masters, B.R. Digital Image Processing, Third Edition. *Journal of Biomedical Optics*. 2009. 14(2):029901.

Grady, L. Random walks for image segmentation. *IEEE Transactions on Pattern Analysis and Machine Intelligence*. 2006. 28(11):1768–1783.

Graichen, H., Jakob, J., Eisenhart-Rothe, Englmeier, K.H., Reiser, M. and Eckstein, F. Validation of cartilage volume and thickness measurements in the human shoulder with quantitative magnetic resonance imaging. *Osteoarthritis and Cartilage*. 2003. 11(7):475–482.

Grau, V., Mewes, A.U.J., Alcaniz, M., Kikinis, R. and Warfield, S.K. Improved watershed transform for medical image segmentation using prior information. *IEEE Transactions on Medical Imaging*. 2004. 23(4):447–458.

Gray, M.L., Eckstein, F., Peterfy, C., Dahlberg, L., Kim, Y.J. and Sorensen, A.G. Toward imaging biomarkers for osteoarthritis. *Clinical Orthopaedics and Related Research*. 2004. 427:175–181.

Gupta, S. and Kaur, Y. Review of Different Local and Global Contrast Enhancement Techniques for a Digital Image. *International Journal of Computer Applications*. 2014. 100(18):18–23.

Haugen, I.K. and Bøyesen, P. Imaging modalities in hand osteoarthritis - status and perspectives of conventional radiography, magnetic resonance imaging, and ultrasonography. *Arthritis Research and Therapy*. 2011. 13(6):248.

Heuer, F., Sommers, M., Reid, J.B. and Bottlang, M. Estimation of cartilage thickness from joint surface scans: Comparative analysis of computational methods. *American Society of Mechanical Engineers, Bioengineering Division (Publication) BED*. 2001. 50:569–570.

Hildebrand, T. and Rüegsegger, P. A new method for the model-independent assessment of thickness in three-dimensional images. *Journal of Microscopy*. 1997. 185(1):67–75.

Hochberg, M.C., Zhan, M. and Langenberg, P. The rate of decline of joint space width inpatientswithosteoarthritis of the knee: A systematic review and meta-analysis of randomized placebo-controlled trials of chondroitin sulfate. *Current Medical Research and Opinion*. 2008. 24(11):3029–3035.

Huang, S.C., Cheng, F.C. and Chiu, Y.S. Efficient contrast enhancement using adaptive gamma correction with weighting distribution. *IEEE Transactions on Image Processing*. 2013. 22(3):1032–1041.

Hunter, D.J., Zhang, Y.Q., Tu, X., LaValley, M., Niu, J.B., Amin, S., Guermazi, A., Genant, H., Gale, D. and Felson, D.T. Change in joint space width: Hyaline articular cartilage loss or alteration in meniscus? *Arthritis and Rheumatism*. 2006. 54(8):2488–2495.

van Ijsseldijk, E.A., Valstar, E.R., Stoel, B.C., Nelissen, R.G.H.H., Baka, N., van't Klooster, R. and Kaptein, B.L. Three dimensional measurement of minimum joint space width in the knee from stereo radiographs using statistical shape models. *Bone and Joint Research*. 2016. 5(8):320–327.

Ismail, W.Z.W. and Sim, K.S. Contrast enhancement dynamic histogram equalization for medical image processing application. *International Journal of Imaging Systems and Technology*. 2011. 21(3):280–289.

Jones, S.E., Buchbinder, B.R. and Aharon, I. Three-dimensional mapping of cortical thickness using Laplace's equation. *Human Brain Mapping*. 2000. 11(1):12–32.

Kandhway, P., Bhandari, A.K. and Singh, A. A novel reformed histogram equalization based medical image contrast enhancement using krill herd optimization. *Biomedical Signal Processing and Control*. 2020. 56(2020):101677.

Kass, M., Witkin, A. and Terzopoulos, D. Snakes: Active contour models. *International journal of computer vision*. 1988. 1(4):321–331.

Kauffmann, C., Gravel, P., Godbout, B., Gravel, A., Beaudoin, G., Raynould, J.P., Martel-Pelletier, J., Pelletier, J.P. and de Guise, J.A. Computer-aided method for quantification of cartilage thickness and volume changes using MRI: Validation study using a synthetic model. *IEEE Transactions on Biomedical Engineering*. 2003. 50(8):978–988.

Kellgren, J.H. and Lawrence, J.S. Radiological assessment of osteo-arthrosis. *Annals of the rheumatic diseases*. 1957. 16(4):494–502.

Kikinis, R., Shenton, M.E., Losifescu, D.V., McCarley, R.W., Saiviroonporn, P., Hokama, H.H., Robatino, A., Metcalf, D., Wible, C.G., Portas, C.M., Donnino, R.M. and Jolesz, F.A. A digital brain atlas for surgical planning, model-driven segmentation, and teaching. *IEEE Transactions on Visualization and Computer Graphics*. 1996. 2(3):232–241.

Kim, M.J., Park, T., Lee, S., Jung, H.Y. and Yun, I.D. Semi-automatic segmentation of knee cartilage in longitudinal MR images by seed transfer. *2nd International Conference on Electrical, Communication and Computer Engineering, ICECCE 2020*. June 12-13, 2020. Istanbul: IEEE. 2020. 2–7.

Kim, Y.T. Contrast enhancement using brightness preserving bi-histogram equalization. *IEEE Transactions on Consumer Electronics*. 1997. 43(1):1–8.

Kittler, J. On the accuracy of the Sobel edge detector. *Image and Vision Computing*. 1983. 1(1):37–42.

Koo, S., Gold, G.E. and Andriacchi, T.P. Considerations in measuring cartilage thickness using MRI: Factors influencing reproducibility and accuracy. *Osteoarthritis and Cartilage*. 2005. 13(9):782–789.

Kraus, V.B., Burnett, B., Coindreau, J., Cottrell, S., Eyre, D., Gendreau, M., Gardiner, J., Garnero, P., Hardin, J., Henrotin, Y., Heinegard, D., Ko, A., Lohmander, L.S., Matthews, G., Menetski, J., Moskowitz, R., Persiani, S., Poole, A.R. and Todman, M. Application of biomarkers in the development of drugs intended for the treatment of osteoarthritis. *Osteoarthritis and Cartilage*. 2011. 19(5):515–542.

Kumar Singh, P., Sharma, G. and Kumar Pandey, P. Watershed Algorithm and Adaptive Threshold Canny Edge Detection Based Automatic Segmentation of Tibio Femoral Cartilage from MRI Images. *Biosciences, Biotechnology Research Asia*. 2017. 14(2):843–852.

Lawson, B., Putnam, W., Nicol, K., Archibald, G., Mackillop, J., Conter, H. and Frail, D. Managing osteoarthritis. Medication use among seniors in the community. *Canadian Family Physician*. 2004. 50:1664–1670.

Lee, H.S., Kim, H.A., Kim, H., Hong, H., Yoon, Y.C. and Kim, J. Multi-atlas segmentation of the cartilage in knee MR images with sequential volume- and bone-mask-based registrations. *Medical Imaging 2016: Computer-Aided Diagnosis*. 2016. 9785:97853H.

Lee, J.G., Gumus, S., Moon, C.H., Kwoh, C.K., Bae, K.T. Fully automated segmentation of cartilage from the MR images of knee using a multi-atlas and local structural analysis method. *Medical Physics*. 2014. 41(9):092303.

León, M. and Escalante-Ramirez, B. Segmentation of knee cartilage by using a hierarchical active shape model based on multi-resolution transforms in magnetic resonance images. *IX International Seminar on Medical Information Processing and Analysis*. 2013. 8922:892214.

Lim, M. and Hacihaliloglu, I. Segmentation of knee MRI using structure enhanced local phase filtering. *Medical Imaging 2016: Computer-Aided Diagnosis*. 2016. 9785:97853B.

Liu, F., Zhou, Z., Jang, H., Samsonov, A., Zhao, G. and Kijowski, R. Deep convolutional neural network and 3D deformable approach for tissue segmentation in musculoskeletal magnetic resonance imaging. *Magnetic Resonance in Medicine*. 2018. 79(4):2379–2391.

Liu, F., Zhou, Z., Samsonov, A., Blankenbaker, D., Larison, W., Kanarek, A., Lian, K., Kambhampati, S. and Kijowski, R. Deep learning approach for evaluating knee MR images: Achieving high diagnostic performance for cartilage lesion detection. *Radiology*. 2018. 289(1):160–169.

Liu, Y., Jin, D., Li, C., Janz, K.F., Burns, T.L., Torner, J.C., Levy, S.M., Saha, P.K. A robust algorithm for thickness computation at low resolution and its application to in Vivo trabecular bone CT imaging. *IEEE Transactions on Biomedical Engineering*. 2014. 61(7):2057–2069.

Lockard, C.A., Stake, I.K., Brady, A.W., DeClercq, M.G., Tanghe, K.K., Douglass, B.W., Nott, E., Ho, C.P. and Clanton, T.O. Accuracy of MRI-Based Talar Cartilage Thickness Measurement and Talus Bone and Cartilage Modeling: Comparison with Ground-Truth Laser Scan Measurements. *Cartilage*. 2020. 194760352097677.

Lorigo, L.M., Faugeras, O., Grimson, W.E.L., Keriven, R. and Kikinis, R. Segmentation of bone in clinical knee MRI using texture-based geodesic active contours. In: *Lecture Notes in Computer Science (including subseries Lecture Notes in Artificial Intelligence and Lecture Notes in Bioinformatics)*. 1998. 1195–1204.

Luque-Chang, A., Cuevas, E., Cisneros, M.A.P., Fausto, F., Gonzalez, A., V. and Sarkar, R. Moth Swarm Algorithm for Image Contrast Enhancement. *Knowledge-Based Systems*. 2021. 212:106607.

Lynch, J.A., Zaim, S., Zhao, J., Stork, A., Peterfy, C.G. and Genant, H.K. Cartilage segmentation of 3D MRI scans of the osteoarthritic knee combining user knowledge and active contours. *Medical Imaging 2000: Image Processing*. 2000. 925–935.

Mahapatra, D. Cardiac image segmentation from cine cardiac MRI using graph cuts and shape priors. *Journal of Digital Imaging*. 2013. 26(4):721–730.

Maier, A., Syben, C., Lasser, T. and Riess, C. A gentle introduction to deep learning in medical image processing. *Zeitschrift fur Medizinische Physik*. 2019. 29(2):86–101.

Maier, J., Black, M., Bonaretti, S., Bier, B., Eskofier, B., Choi, J.H., Levenston, M., Gold, G., Fahrig, R. and Maier, A. Comparison of Different Approaches for Measuring Tibial Cartilage Thickness. *Journal of integrative bioinformatics*. 2017. 14(2):1–11.

Maqsood, S. and Javed, U. Multi-modal Medical Image Fusion based on Two-scale Image Decomposition and Sparse Representation. *Biomedical Signal Processing and Control*. 2020. 57(2020):101810.

Memari, N. and Moghbel, M. Computer-Aided Diagnosis (CAD) of Knee Osteoarthritis based on Magnetic Resonance Imaging for Quantitative Pathogenesis Analysis and Visualization. *ISCAIE 2020 - IEEE 10th Symposium on Computer Applications and Industrial Electronics*. April 18-19, 2020. Penang: IEEE. 2020. 192–197.

Millington, S.A., Grabner, M., Wozelka, R., Anderson, D.D., Hurwitz, S.R. and Crandall, J.R. Quantification of ankle articular cartilage topography and thickness using a high resolution stereophotography system. *Osteoarthritis and Cartilage*. 2007. 15(2):205–211.

Mittal, A., Moorthy, A.K. and Bovik, A.C. No-reference image quality assessment in the spatial domain. *IEEE Transactions on Image Processing*. 2012. 21(12):4695–4708.

Mittal, A., Soundararajan, R. and Bovik, A.C. Making a ‘completely blind’ image quality analyzer. *IEEE Signal Processing Letters*. 2013. 20(3):209–212.

Neumann, G., Hunter, D., Nevitt, M., Chibnik, L.B., Kwoh, K., Chen, H., Harris, T., Satterfield, S. and Duryea, J. Location specific radiographic joint space width for osteoarthritis progression. *Osteoarthritis and Cartilage*. 2009. 17(6):761–765.

Newton, M.D., Junginger, L. and Maerz, T. Automated MicroCT-based bone and articular cartilage analysis using iterative shape averaging and atlas-based registration. *Bone*. 2020. 137(November):115417.

Nyee, W.J., Hum, Y.C., Chai, T.Y. and Tee, Y.K. The Design and Development of Automated Knee Cartilage Segmentation Framework. *Proceedings of the 2019 IEEE International Conference on Signal and Image Processing Applications, ICSIPA 2019*. September 17-19, 2019. Kuala Lumpur: IEEE. 2019. 84–88.

MacQueen, J. Some methods for classification and analysis of multivariate observations. *Proceedings of the fifth Berkeley symposium on mathematical statistics and probability*. December 27, 1965 - January 7, 1966. Statistical Laboratory University of California: Universiti of Carlifornia Press. 1967. 1(14):281–297.

Öztürk, C. N., and Albayrak, S. Automatic segmentation of cartilage in high-field magnetic resonance images of the knee joint with an improved voxel-classification-driven region-growing algorithm using vicinity-correlated subsampling. *Computers in Biology and Medicine*. 2016. 72:90–107.

Pakin, S.K., Tamez-Pena, J.G., Totterman, S. and Parker, K.J. Segmentation, surface extraction, and thickness computation of articular cartilage. *Medical Imaging 2002*. 2002. 155.

Park, G.H., Cho, H.H. and Choi, M.R. A contrast enhancement method using dynamic range separate histogram equalization. *IEEE Transactions on Consumer Electronics*. 2008. 54(4):1981–1987.

Patil, S.G., Zheng, Y.P., Wu, J.Y. and Shi, J. Measurement of depth-dependence and anisotropy of ultrasound speed of bovine articular cartilage in vitro. *Ultrasound in Medicine and Biology*. 2004. 30(7):953–963.

Pizer, S.M., Amburn, E.P., Austin, J.D., Cromartie, R., Geselowitz, A., Greer, T., Romeny, B.t.H., Zimmerman, J.B. and Zuiderveld, K. Adaptive Histogram Equalization and Its Variations. *Computer vision, graphics, and image processing*. 1987. 39(3):355–368.

Prasoon, A., Igel, C., Loog, M., Lauze, F., Dam, E.B. and Nielsen, M. Femoral cartilage segmentation in Knee MRI scans using two stage voxel classification. *Proceedings of the Annual International Conference of the IEEE Engineering in Medicine and Biology Society, EMBS*. July 3-7, 2013. Osaka: IEEE. 2013. 5469–5472.

Raj, A., Vishwanathan, S., Ajani, B., Krishnan, K. and Agarwal, H. Automatic knee cartilage segmentation using fully volumetric convolutional neural networks for evaluation of osteoarthritis. *Proceedings - International Symposium on Biomedical Imaging*. April 4-7, 2018. Washington: IEEE. 2018. 851–854.

Raynauld, J.P., Pelletier, J.P., Delorme, P., Dodin, P., Abram, F. and Martel-Pelletier, J. Bone curvature changes can predict the impact of treatment on cartilage volume loss in knee osteoarthritis: Data from a 2-year clinical trial. *Rheumatology (United Kingdom)*. 2017. 56(6):989–998.

Reichmann, W.M., Maillefert, J.F., Hunter, D.J., Katz, J.N., Conaghan, P.G. and Losina, E. Responsiveness to change and reliability of measurement of radiographic joint space width in osteoarthritis of the knee: A systematic review. *Osteoarthritis and Cartilage*. 2011. 19(5):550–556.

Reynolds, D. Gaussian Mixture Models. *Encyclopedia of Biometrics*. 2009. (2): 659–663.

Rogowska, J., Bryant, C.M. and Brezinski, M.E. Cartilage thickness measurements from optical coherence tomography. *Journal of the Optical Society of America A*. 2003. 20(2):357.

Rohlfing, T., Brandt, R., Menzel, R., Russakoff, D.B. and Maurer, C.R.J. Quo Vadis, Atlas-Based Segmentation? In: *Handbook of Biomedical Image Analysis*. 2005. 435–486.

Rosenfeld, J.A. *Handbook of Women's Health*. Cambridge University : Cambridge University Press. 2010.

Rundo, L., Tangherloni, A., Nobile, M., Militello, C., Besozzi, D., Mauri, G., Cazzaniga, P. MedGA: A novel evolutionary method for image enhancement in medical imaging systems. *Expert Systems with Applications*. 2019. 119:387–399.

Schaefer, L.F., Sury, M., Yin, M., Jamieson, S., Donnell, I., Smith, S.E., Lynch, J.A., Nevitt, M.C. and Duryea, J. Quantitative measurement of medial femoral knee cartilage volume – analysis of the OA Biomarkers Consortium FNIH Study cohort. *Osteoarthritis and Cartilage*. 2017. 25(7):1107–1113.

Schiphof, D., Oei, E.H.G., Hofman, A., Waarsing, J.H., Weinans, H. and Bierma-Zeinstra, S.M.A. Sensitivity and associations with pain and body weight of an MRI definition of knee osteoarthritis compared with radiographic Kellgren and Lawrence criteria: A population-based study in middle-aged females. *Osteoarthritis and Cartilage*. 2014. 22(3):440–446.

Schmitz, R.J., Wang, H.M., Polprasert, D.R., Kraft, R.A. and Pietrosimone, B.G. Evaluation of knee cartilage thickness: A comparison between ultrasound and magnetic resonance imaging methods. *Knee*. 2017. 24(2):217–223.

Shah, R.F., Martinez, A.M., Pedoia, V., Majumdar, S., Vail, T.P. and Bini, S.A.B. Variation in the Thickness of Knee Cartilage. The Use of a Novel Machine Learning Algorithm for Cartilage Segmentation of Magnetic Resonance Images. *Journal of Arthroplasty*. 2019. 34(10):2210–2215.

Shan, L., Charles, C. and Niethammer, M. Automatic multi-atlas-based cartilage segmentation from knee MR images. *Proceedings - International Symposium on Biomedical Imaging*. May 2-5, 2012. Barcelona: IEEE . 2012. 1028–1031.

Shan, L., Zach, C., Charles, C. and Niethammer, M. Automatic atlas-based three-label cartilage segmentation from MR knee images. *Medical Image Analysis*. 2014. 18(7):1233–1246.

Smith, J.J., Sorensen, A.G. and Thrall, J.H. Biomarkers in imaging: Realizing radiology's future. *Radiology*. 2003. 227(3):633–638.

Soh, S.S., Tan, T.S., Sim, S.Y., Chuah, Z.E., Mazenan, M.N. and Leong, K.M. Magnetic resonance image segmentation for knee osteoarthritis using active shape models. *BMEiCON 2014 - 7th Biomedical Engineering International Conference*. November 26-28, 2014. Fukuoka, Japan:IEEE. 2014. 1–5.

Solloway, S., Hutchinson, C.E., Waterton, J.C. and Taylor, C.J. The use of active shape models for making thickness measurements of articular cartilage from MR images. *Magnetic Resonance in Medicine*. 1997. 37(6):943–952.

Stammberger, T., Eckstein, F., Michaelis, M., Englmeier, H. and Reiser, M. Interobserver reproducibility of quantitative cartilage measurements: Comparison of B-spline snakes and manual segmentation. *Magnetic Resonance Imaging*. 1999. 17(7):1033–1042.

Steinmeyer, J., Bock, F., Stöve, J., Jerosch, J. and Flechtenmacher, J. Pharmacological treatment of knee osteoarthritis: Special considerations of the new German guideline. *Orthopedic Reviews*. 2018. 10(4).

Steppacher, S.D., Hanke, M.S., Zurmühle, C.A., Haefeli, P.C., Klenke, F.M. and Tannast, M. Ultrasonic cartilage thickness measurement is accurate, reproducible, and reliable - Validation study using contrast-enhanced micro-CT. *Journal of Orthopaedic Surgery and Research*. 2019. 14(1):1–10.

Su, H., Xing, F., Kong, X., Xie, Y., Zhang, S. and Yang, L. Robust cell detection and segmentation in histopathological images using sparse reconstruction and stacked denoising autoencoders. *Advances in Computer Vision and Pattern Recognition*. 2017. 257–278.

Tamez-Peña, J.G. Farber, J., González, P.C., Schreyer, E. Schneider, E. and Totterman, S. Unsupervised segmentation and quantification of anatomical knee features: Data from the osteoarthritis initiative. *IEEE Transactions on Biomedical Engineering*. 2017. 59(4):1177–1186.

Tang, J., Millington, S., Acton, S.T., Crandall, J. and Hurwitz, S. Surface extraction and thickness measurement of the articular cartilage from MR images using directional gradient vector flow snakes. *IEEE Transactions on Biomedical Engineering*. 2006. 53(5):896–907.

Teh, V., Sim, K.S. and Wong, E.K. Contrast enhancement of CT brain images using gamma correction adaptive extreme-level eliminating with weighting distribution. *International Journal of Innovative Computing, Information and Control*. 2018. 14(3):1029–1041.

Tilson, L. V., Excell, P.S. and Green, R.J. A generalisation of the Fuzzy c-Means clustering algorithm. *International Symposium on Geoscience and Remote Sensing: Moving Towards the 21st Century.* September 12-16, 1988. United Kingdom: IEEE. 1988. 3:1783–1784.

Torp-Pedersen, S., Bartels, E.M., Wilhjelm, J. and Bliddal, H. Articular cartilage thickness measured with us is not as easy as it appears: A systematic review of measurement techniques and image interpretation. *Ultraschall in der Medizin*. 2011. 32(1):54–61.

von Tycowicz, C., Ambellan, F., Mukhopadhyay, A. and Zachow, S. An efficient Riemannian statistical shape model using differential coordinates: With application to the classification of data from the Osteoarthritis Initiative. *Medical Image Analysis*. 2018. 43:1–9.

Veerapen, K., Wigley, R.D. and Valkenburg, H. Musculoskeletal pain in Malaysia: A COPCORD survey. *Journal of Rheumatology*. 2007. 34(1):207–213.

Vilimek, D., Kubicek, J., Penhaker, M., Oczka, D., Augustynek, M. and Cerny, M. Current Automatic Methods for Knee Cartilage Segmentation: A Review. *Proceedings - European Workshop on Visual Information Processing, EUVIP*. October 28-31, 2019. Roma, Italy: IEEE. 2019. 117–122.

Vincent, K. R., Conrad, B. P., Fregly, B. J. and Vincent, H. K. The pathophysiology of osteoarthritis: a mechanical perspective on the knee joint. *PM&R*. 2013. 4(5):1–11.

Vinet, L. and Zhedanov, A. A ‘missing’ family of classical orthogonal polynomials. *Journal of Physics A: Mathematical and Theoretical*. 2011. 44(8):223–248.

Wallace, I.J., Worthington, S., Felson, D.T., Jurmain, R.D., Wren, K.T., Maijanen, H., Woods, R.J. and Lieberman, D.E. Knee osteoarthritis has doubled in prevalence since the mid-20th century. *Proceedings of the National Academy of Sciences of the United States of America*. August 29, 2017. USA: National Academy of Sciences. 2017. 114(35): 9332–9336.

Wang, P., He, X., Li, Y., Zhu, X., Chen, W. and Qiu, M. Automatic knee cartilage segmentation using multi-feature support vector machine and elastic region growing for magnetic resonance images. *Journal of Medical Imaging and Health Informatics*. 2016. 6(4):948–956.

Wang, Z. and Bovik, A.C. Modern image quality assessment. *Synthesis Lectures on Image, Video, and Multimedia Processing*. 2005. 3(1):1–156.

Wang, Z., Bovik, A.C., Sheikh, H.R. and Simoncelli, E.P. Image quality assessment: From error visibility to structural similarity. *IEEE Transactions on Image Processing*. 2004. 13(4):600–612.

Wirth, W., Maschek, S., Ladel, C., Guehring, H., Michaelis, M. and Eckstein, F. Progressor rates of femorotibial cartilage loss stratified by radiographic disease stage, 1 to 4-year observation intervals, and MRI protocols – Data from the osteoarthritis initiative. *Osteoarthritis and Cartilage*. 2019. 27(2019):S53–S54.

Xu, C. and Prince, J.L. Snakes, shapes, and gradient vector flow. *IEEE Transactions on Image Processing*. 1998. 7(3):359–369.

Yang, C., Zhang, L., Lu, H., Ruan, X. and Yang, M-H. Saliency detection via graph-based manifold ranking. *Proceedings of the IEEE Computer Society Conference on Computer Vision and Pattern Recognition*. June 23-28, 2013. Washington: IEEE. 2013. 3166–3173.

Yao, Z., Lai, Z. and Wang, C. Image Enhancement Based on Equal Area Dualistic Sub-image and Non-parametric Modified Histogram Equalization Method. *Proceedings - 2016 9th International Symposium on Computational Intelligence and Design, ISCID 2016*. December 10-11, 2016. Hangzhou: IEEE. 2016. 1(1):447–450.

Yezzi, A.J. and Prince, J.L. An Eulerian PDE Approach for Computing Tissue Thickness. *IEEE Transactions on Medical Imaging*. 2003. 22(10):1332–1339.

Yin, Y., Zhang, X., Williams, R., Wu, X., Anderson, D.D. and Sonka, M. LOGISMOS-layered optimal graph image segmentation of multiple objects and surfaces: Cartilage segmentation in the knee joint. *IEEE Transactions on Medical Imaging*. 2010. 29(12):2023–2037.

Zhang, K., Deng, J. and Lu, W. Segmenting human knee cartilage automatically from multi-contrast MR images using support vector machines and discriminative random fields. *Proceedings - International Conference on Image Processing, ICIP*. September 11-14, 2011. Belgium: IEEE. 2011. 721–724.

Zhang, Z., Duan, C., Lin, T., Zhou, S., Wang, Y. and Gao, X. GVFOM: a novel external force for active contour based image segmentation. *Information Sciences*. 2020. 506:1–18.

Zhou, D., Weston, J., Gretton, A., Bousquet, O. and Schölkopf, B. Ranking on data manifolds. *Advances in Neural Information Processing Systems*. 2004. 16:169-176.

Zuiderveld, K. Contrast Limited Adaptive Histogram Equalization. *Graphics Gems*. 1994. 474–485.

LIST OF PUBLICATIONS

Indexed Journal

1. **Sia, J.S.S.Y.**, Tan. T.S., Yahya, A, Foh, M.T.T. and Sia, J.Y.X. 2021. Mini Kirsch Edge Detection and Its Sharpening Effect. *Indonesian Journal of Electrical Engineering and Informatics (IJEEI), 9*(1), 228-244. (Scopus)

2. **Sia, J.S.S.Y.** et al. 2020. Prominent Region of Interest Contrast Enhancement for Knee MR Images: Data from the OAI. *Jurnal Kejuruteraan, 32*(3), 145-155. (WOS, ESCI)

3. **Sia, J.S.S.Y.** et al. 2020. K-means Clustering in Knee Cartilage Classification: Data from the OAI. *Indonesian Journal of Electrical Engineering and Informatics (IJEEI), 8*(2), 320-330. (Scopus)

4. **Sia, J.S.S.Y.** et al. 2021. Magnetic Resonance Imaging-Based Estimation of Knee Cartilage Thickness with MATLAB. *Jurnal Kejuruteraan,* 33(4). (In press, ESCI)

Non-Indexed Conference Proceeding

1. Sia, J.S.S.Y. et al. 2020. Minimal Interactive Knee Cartilage Segmentation Model. 8th International Graduate Conference on Engineering, Science and Humanities. August 17-19, 2020. School of Graduates Studies. (ISSN: 2735-055x)